Development of a Stable and Buffered Reference Electrode for Binary Molten Chlorides Salts

Carlos Mejia[a,*], Nicholas Christensen[a], Ricardo Rodriguez Ceron[a], and Devin Rappleye[a]

[a] Department of Chemical Engineering, Brigham Young University, Provo, Utah 84602 USA

* Corresponding author: carlos_mejia@byu.edu

Abstract

The development of stable and buffered reference electrodes (REs) is crucial for molten salt electrochemistry, particularly in pyrochemical processing, such as electrorefining. These REs must maintain a stable potential to ensure precise control over electrorefining processes by preventing unwanted shifts in the potential that could lead to impurity deposition. This study evaluated metal chlorides and metal oxides as potential candidates for REs, with their stability assessed via electrochemical methods over extended durations. While metal chloride-based REs exhibited stable potential behavior over time, their response followed the Nernst equation, leading to potential shifts with varying concentrations of oxidized species. Metal oxide-based REs were explored to address the need for both stability and concentration-independent potential. These REs demonstrated the ability to maintain a constant potential regardless of concentration changes. The introduction of this metal oxide-based RE presents a promising advancement for use in binary chloride molten salts, offering robust, stable performance in electrorefining applications, particularly in the electrorefining of plutonium within equimolar sodium chloride and potassium chloride (NaCl-KCl) molten salt systems.

Keywords

Molten salts, metal chlorides, metal oxides, reference electrode, cyclic voltammetry, electrochemical impedance spectroscopy, chronopotentiometry

Highlights

- $NiCl_2$ provided stability, but potential varied due to challenges with saturation.
- Developed stable, buffered NiO-based reference electrodes (REs) for molten salts.
- Demonstrated RE potentials independent of metal oxide added.
- Validated RE stability using EIS, CP-OCP, and CV over multiple days.
- NiO-based REs showed minimal drift and variability compared to Ag/AgCl reference systems.

1. Introduction

Molten chloride salts are used in electrowinning lithium and magnesium metals [1–3], electrorefining of actinide metals [4,5], advanced nuclear reactors [6,7], namely molten salt reactors (MSRs),

and other critical material and energy production processes, as reviewed elsewhere [8]. An electrochemical sensor can aid in process monitoring, corrosion control, and nuclear material accountancy in each application [9]. The accuracy of the electrochemical sensor depends upon the stability and reproducibility of the reference electrode (RE). In the applications given, the stability of a RE in an electrochemical sensor needs to be maintained in the order of days to weeks for electrowinning and electrorefining and months to years for MSRs. Hence, increasing the stability of REs in molten chlorides will improve process control and efficiency and provide a reliable means of nuclear material accountancy.

Most REs used in molten chloride salts are custom-made, leading to variability within and across different studies, particularly because they are often concentration-dependent due to the lack of saturation. During the construction of a RE, salt can adhere to the walls of the RE membrane, potentially failing to achieve the expected reference potential due to the missing targeted concentration in the molten bath within the RE. This can be a significant source of error in lab-scale experiments where the RE compartment may contain 1 g or less of total salt and 1 wt.% of the reference analyte (e.g., AgCl). Furthermore, the quality of the salt is another critical factor, as any residual moisture can react with the reference analyte to form an insoluble oxide precipitate, impacting the concentration within the RE. Additionally, selective vaporization of the salts presents a significant challenge. Improper sealing of the RE membrane can allow analyte vaporization or recrystallization on cooler areas of the RE wire, driven by the high-temperature gradient between the molten salt inside the RE and the ambient environment. These challenges, including variability in concentration, salt quality, and improper sealing, can result in inconsistencies in RE potentials and performance.

Quasi-REs (QREs) are widely used in electrochemical applications due to their ease of adaptation to various molten salts [10–13], and their stability is serviceable in short-term (≤ 1 day) voltammetry measurements, as previously examined [14]. A limitation of QREs is their inability to provide a well-defined potential (i.e., their potential depends on the concentration of analyte(s) and/or impurities in the main bath), which can reduce their applicability in electrorefining processes where concentration in the main salt bath varies and precise potential control is needed. On the other hand, metal chloride-based REs encased in a membrane are commonly used in molten salts and offer more stable, well-defined potentials due to the isolation of the reference salt bath from the main bath. The silver-silver chloride (Ag/AgCl) system is the most established [13,15–20]. There are other metal chloride-based REs that include tungsten-cobalt chloride ($W/CoCl_2$) [21], magnesium-magnesium chloride ($Mg/MgCl_2$) [22], and gadolinium-gadolinium chloride ($Gd/GdCl_3$) [23] for chloride salts and nickel-nickel fluoride (Ni/NiF_2) for fluoride salts [24]. The potential stability of Ag/AgCl REs, utilizing alumina, magnesia, boron nitride, mullite, and quartz membranes, has been investigated in chloride melts for reproducibility and life-long duration [25–29]. However, when incorporated in an equimolar mixture of sodium chloride and potassium chloride (NaCl-KCl) or other molten salts, Ag/AgCl REs cannot form a solid film

and saturated solution, as in aqueous solutions due to the high solubility of AgCl in molten chlorides. Hence, Ag/AgCl REs still exhibit some variation in redox potentials due to concentration variations from imprecise addition of AgCl, loss of AgCl (e.g., vaporization, diffusion through the membrane), and dendrite formation driven by thermal gradients [30].

NaCl-KCl molten salts are commonly used in electrochemical processes (e.g., electrorefining) with metals requiring high operating temperatures, such as plutonium [31,32]. However, the incorporation of a stable RE in these systems has yet to be implemented. The electrochemistry of plutonium and its surrogates has been studied using Ag/AgCl REs, but the electrochemical data can vary significantly between research groups [33–39]. These variations arise partly from differences in potential, which are influenced by concentration differences in Ag/AgCl REs. Therefore, there is a need to develop a repeatable and stable, buffered RE capable of forming a saturated phase for use in binary chloride molten salts that operate at high temperatures.

Our group has developed a saturated and buffered RE (SRE) using nickel-nickel chloride ($Ni/NiCl_2$) in single chloride systems, demonstrating that $NiCl_2$ offers greater stability compared to AgCl due to the saturation phase of $NiCl_2$ in lithium chloride (LiCl) and calcium chloride ($CaCl_2$) molten salts [40]. Nickel-based REs, such as those employing nickel hydroxide ($Ni(OH)_2$) in hydroxide salts and nickel oxide (NiO) in chloride and carbonate salts, have been applied in various applications [10,41,42]. Despite the common use of Ni/NiO RE in molten LiCl, no study was found characterizing its stability and chemistry [43,44]. The stability of a saturated phase has not yet been evaluated for $NiCl_2$ or NiO-based REs in NaCl-KCl molten salts.

When developing a SRE for use in NaCl-KCl molten salts, three key criteria must be considered, each of which could lead to advancements in electrorefining processes. These criteria include: (1) an analyte with a high melting point, (2) a high density, and (3) solubility in NaCl-KCl molten salts. $NiCl_2$ and NiO satisfy these conditions. A higher melting point and density are desired to allow the formation of a secondary phase at the bottom of the RE to buffer the reference solution when saturated at the operating temperature. Additionally, the analyte must be soluble in NaCl-KCl to facilitate ionization and redox activity within the RE. The potential of the RE is based on the Nernst equation, as shown in the following expression:

$$E = E_i^0 - \frac{RT}{nF} \ln \frac{a_{R,i}}{a_{O,i}}, \quad (1)$$

where E is the electrode potential relative to the RE, E_i^0 is the standard potential of the redox couple, R is the ideal gas constant, T is the absolute temperature, n is the number of electrons transferred in the redox reaction, F is the Faraday's constant, and $a_{R,i}$ and $a_{O,i}$ represent the activities of the reducing and oxidizing species, respectively, in equilibrium. Thus, assuming ideal behavior, a saturated analyte can

be advantageous for developing stable SREs due to the consistent concentration of the oxidized species.

In this study, the stability and buffering capability of the developed SREs, using metal chlorides and metal oxides in NaCl-KCl molten salts, were evaluated electrochemically through four techniques: electrochemical impedance spectroscopy (EIS), chronopotentiometry (CP), open circuit potential (OCP), and cyclic voltammetry (CV). The stability of the developed REs was evaluated by forming an alloy via sodium (Na) deposition onto a platinum (Pt) working electrode (WE), which provided the most accurate approach for quantitatively assessing RE stability over time. Additionally, CV data quantitively evaluated RE stability by examining the overlap of data collected over time, while EIS allowed for quantifying both the molten bath conditions and the state of the WE. The full electrochemical window of NaCl-KCl was measured using tungsten (W) electrodes with the developed REs.

2. Experimental

2.1. Materials

Sodium chloride (NaCl, ACS grade, 99.0%, Thermo Scientific Chemicals) and potassium chloride (KCl, ACS grade, 99.0-100.5%, Thermo Scientific Chemicals) were dried under vacuum at 503 K for 24 h using a drying oven (Across International, AT32x-316L) to remove residual moisture. Nickel chloride ($NiCl_2$, ultra-dry grade, 99.9%, Thermo Scientific Chemicals), silver chloride (AgCl, extra-pure grade, 99+%, Thermo Scientific Chemicals), and nickel oxide (NiO, Puratronic grade, 99.998%, Thermo Scientific Chemicals) were used as received. All materials were transferred to an argon-filled glovebox (LC Technology Solutions Inc., Project #21-0099) maintained at < 0.1 ppm oxygen and moisture after drying.

2.2. Development of a RE

The compositions of various REs with different analyte concentrations are presented in **Table 1**, and a schematic representation of a RE is shown in **Figure 1**. The mullite tube (McDanel Advanced Ceramic Technologies, MV0160031-06-12) was initially dried under vacuum at 503 K for 12 h using a drying oven, followed by baking at 1173 K for 2 h inside a glovebox equipped with a well furnace. An equimolar mixture of NaCl-KCl and the respective analyte chloride salt for the RE was added to the mullite tube. An alumina two-bore tube (AdValue Technology, AL-T2-N125-N04-12) was employed as both a sheath and a wire straightener for the nickel (Ni, 0.63 mm diameter, 99.5% purity, Thermo Scientific Chemicals) wire or silver (Ag, 0.64 mm diameter, 99.9% purity, Thermo Scientific Chemicals) wire, which was secured to a rubber plug and inserted into the mullite tube. The mullite tube was then heated in a muffle furnace (MTI Corporation, KSL1100XST) until the metal wire dropped, indicating the salts melting at approximately 1073 K. After confirming the melting of the RE salt, the rubber plug was used to properly seal the mullite tube, minimizing the volatilization of the chloride salts and thermal gradients.

Table 1. Composition details of various analytes in equimolar NaCl-KCl for REs examined in this study.

Sample	Analyte	Concentration / mol%
RE1 Ni|Ni^{2+}	$NiCl_2$	20
RE2 Ni|Ni^{2+}	$NiCl_2$	50
RE3 Ag|Ag^{+}	AgCl	4.5
RE4 Ni|Ni^{2+}	$NiCl_2$	4.5
RE5 NiO|O^{2-}	NiO	1.0
RE6 NiO|O^{2-}	NiO	4.5

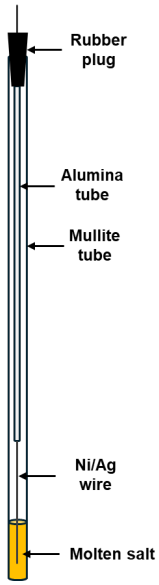

Figure 1. Schematic representation of the fabrication of a RE.

2.3. Molten salt electrochemical setup

An equimolar mixture of NaCl-KCl was placed in an alumina crucible (AdValue Technology, AL-2100) and then inserted into a stainless steel (SS) 304 Faraday cage connected to a ground cable made of Inconel wire. The Faraday cage containing the crucible and salts was transferred to the muffle furnace. An electrochemical lid, specifically designed for this setup, was placed on top of the muffle furnace to position the electrodes accurately. Tungsten (W, 1.5 mm diameter, 99.95% purity, Thermo Scientific Chemicals) and platinum (Pt, 1.0 mm diameter, 99.95% purity, Thermo Scientific Chemicals) were utilized as the WE, with tungsten (W, 3.175 mm diameter, 99.95% purity, Thermo Scientific Chemicals) serving as the counter electrode (CE) throughout the experiment. The electrodes were

sheathed with alumina tubes above the salt to prevent electrical shortages from contacting the SS316 lid. The positions of the electrodes were secured using O-rings. The salts were initially melted at 1073 K, after which the temperature was reduced to the operating temperature of 1023 K. A schematic representation of the electrochemical setup is shown in **Figure 2**.

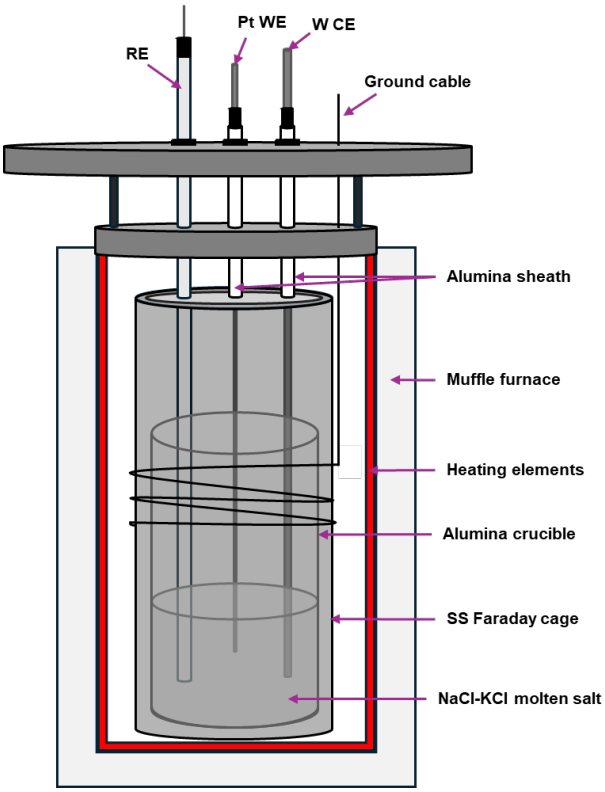

Figure 2. Schematic representation of electrochemical experiment to test stability of several REs.

2.4. Electrochemical stability tests of the RE

A potentiostat (Autolab, PGSTAT302N) was used to conduct electrochemical stability measurements of the RE using electrochemical impedance spectroscopy (EIS), chronopotentiometry-open circuit potential (CP-OCP), and cyclic voltammetry (CV). A script developed in Nova 2.1.7 automated the sequential execution of EIS, CP-OCP, and CV experiments over an extended period using different REs. Data analysis was done using Python to compile and process the collected data. The electrochemical window of NaCl-KCl was characterized using all fabricated REs upon completion of the stability tests.

2.4.1. EIS measurements

EIS was conducted to determine the uncompensated resistance, or solution resistance, of the NaCl-KCl molten salt. This measurement provides insight into the condition of the molten salt, the WE,

and the membrane of the RE. The OCP between the WE and RE was measured initially, followed by EIS performed at 0 V vs. E_{OCP} (the OCP) with a root mean square (RMS) amplitude of 0.01 V over a frequency range from 50 kHz to 1 Hz. A Lissajous plot was used during EIS measurements to verify the stability and linearity of the electrochemical system. The uncompensated resistance (Z_{re}) was determined periodically, specifically when the negative of the imaginary impedance ($-Z_{im}$) is 0 Ω.

2.4.2. CP-OCP measurements

CP was performed on a clean WE by applying a constant current of −0.2 A for 10 s to reduce Na^+ to Na on the WE. Following this, the OCP was monitored for 600 s. The measurement was subject to a criterion where the rate of change of potential (dE/dt) had to be less than or equal to 10^{-6} V s^{-1} for ten consecutive detection points. The OCP measurement was terminated once ten identical OCP values (i.e., $dE/dt < 10^{-6}$ V s^{-1}) were reached, indicating a stable condition.

2.4.3. CV measurements

A linear CV scan was conducted within the electrochemical window of NaCl-KCl using various REs. Four scans were performed at a scan rate of 0.1 V s^{-1} to ensure repeatability. The data from the fourth scan was recorded and reported for the entire measured stability test.

2.5. Characterization of salts

The oxide content of the salts, particularly those containing metal oxide for the RE, was characterized using a back titration method. A Metrohm 916 Ti-Touch titrator was utilized, with 0.1 M hydrochloric acid (HCl, Certified ACS Plus grade, Fisher Chemical) as the standard reagent and 0.1 M sodium hydroxide (NaOH, ACS reagent grade, ≥ 97.0%, pellets, Sigma-Aldrich) as the titrant. More than 10 g of solidified salt was dissolved in 100 mL of ultrapure water, and 5 mL of 0.1 M HCl was added to react with the soluble metal oxides, or any oxides present in the salt. The excess HCl, which did not react with the oxides, was back-titrated with 0.1 M NaOH to the equivalence point. This procedure allowed the oxygen content in the molten salts to be determined.

3. Results and discussion

3.1. Selection of WE for CP-OCP measurements

The OCP value is crucial for determining and validating the stability of the RE. By reducing a metal ion onto the WE surface, a stable potential can be established for comparison to different REs [15,45–47]. W rods were used as both the WE and CE for NaCl-KCl molten salts in the system under investigation. The primary purpose of OCP measurements was to evaluate whether a W WE is suitable for determining the OCP versus the RE when Na^+ is reduced to Na on the WE. Initially, the OCP value of bare W WE and RE was measured (**Figure 3a**). Subsequently, a small current of −0.2 A was applied for 10 s to initiate the reduction of Na^+ onto the W WE (**Figure 3b**). Once sufficient Na was deposited on the W WE, the current was discontinued, and the OCP was measured again (**Figure 3c**).

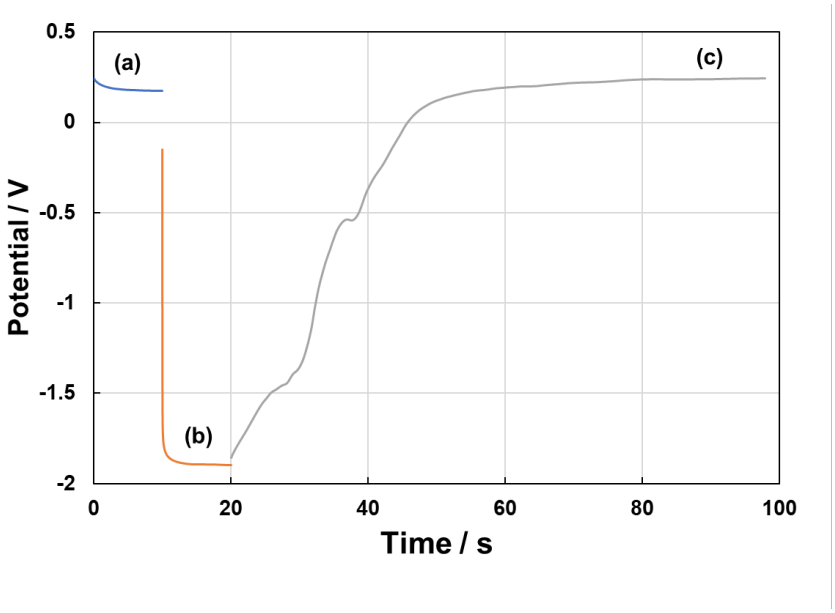

Figure 3. CP-OCP measurements in NaCl-KCl using R5 NiO|O^{2-}, W WE, and W CE. **(a)** OCP of W WE in NaCl-KCl, **(b)** reduction of Na^+ to Na for 10 s at −0.2 A, **(c)** potential relaxation until reaching a stable OCP. WE: 1.5 mm W rod. CE: 3.175 mm W rod.

Upon measuring the OCP, it was observed that the value shifted to a more positive potential, which reflects the potential of the bare W WE. This observation suggests that Na deposits may not adhere firmly to the W WE. Given the high solubility of Na in NaCl-KCl molten salt and its lower density compared to the salt mixture, it is plausible that Na dissolves into the molten salt or floats away, rather than forming a stable coating on the W surface. Consequently, using a W WE does not provide a reliable method for obtaining OCP values for the RE stability testing, as the potential will be mainly dominated by the redox potential of the salt, which can be influenced by the bulk composition of the salt or even trace impurities. Therefore, a different WE must be considered to achieve a stable OCP when Na is deposited on the WE for accurate RE stability testing.

Since we are interested in confirming the stability of the RE using the electrochemical window of NaCl-KCl molten salts without adding a third metal chloride, it is crucial to create a redox pair at the WE that can provide a stable and repeatable potential. A bare inert electrode (e.g., W) does not provide a stable and repeatable potential. A repeatable and stable redox potential can be created using the abundant Na^+ ions present in the molten. The concentration of Na^+ ions in molten, equimolar NaCl-KCl is relatively constant. Furthermore, slight changes in Na^+ ion concentration would have minimal effect on the redox potential due to the high Na^+ concentration. A metal electrode that can interact and form a stable Na-containing coating or deposit would allow a redox couple involving Na^+ ions to set the WE potential. Na can alloy with Pt, forming compounds such as NaPt or $NaPt_2$, depending on the relative concentrations of Na and Pt (**Figure 4**). This alloy formation can be electrochemically induced on the

WE when Na^+ is reduced on the Pt WE. The ability to form alloys on the WE is advantageous for obtaining stable deposits, resulting in reliable OCP values without incorporating a third metal chloride into the NaCl-KCl molten salt system, as demonstrated in **Figure 5c**.

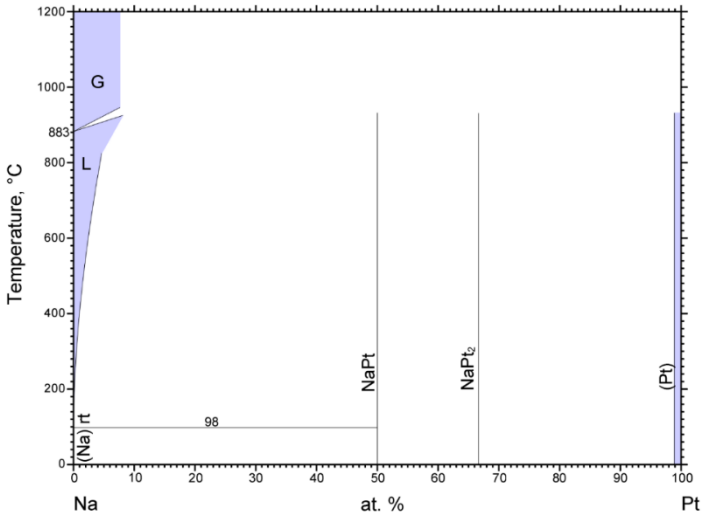

Figure 4. Sodium-platinum binary alloy phase diagram (1990 Okamoto H.) obtained from ASM alloy phase diagram database. Reprinted with permission of ASM International.

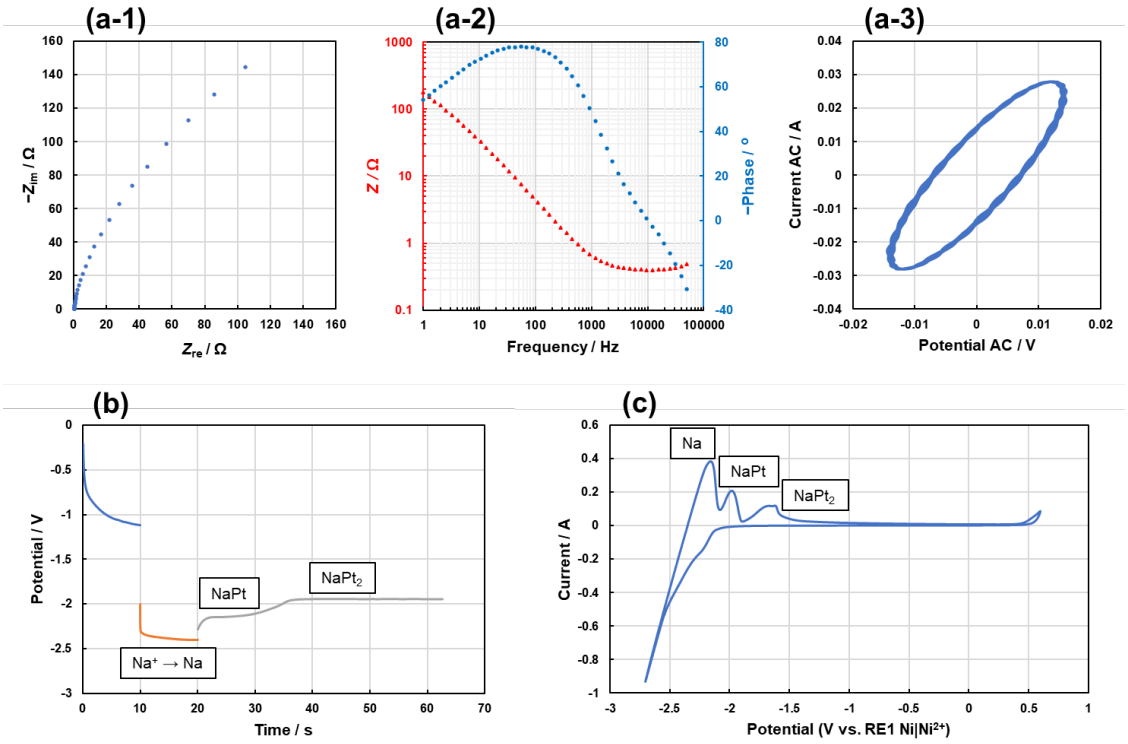

Figure 5. Preliminary results for RE stability test at 1023 K using RE1 $Ni|Ni^{2+}$ with three different electrochemical methods. **(a)** EIS analysis, including **(a-1)** Nyquist plot, **(a-2)** Bode plot, and **(a-3)** Lissajous plot, **(b)** CP-OCP, and **(c)** Full electrochemical window of NaCl-KCl at 0.1 V s^{-1}.

3.2. RE stability test

The three electrochemical techniques (EIS, CP-OCP, and CV) were initially investigated to determine the optimal parameters before running continuous measurements for over three days. Each RE was evaluated individually for stability in a separate equimolar NaCl-KCl molten salt bath. EIS was conducted first to establish the ideal frequency ranges and potentials to apply to generate a Nyquist plot (**Figure 5a-1**), a Bode plot (**Figure 5a-2**), and a Lissajous plot (**Figure 5a-3**). The Nyquist plot was primarily used to determine the solution resistance, while the Lissajous plot indicated that the electrochemical system was stable and linear, as evidenced by the tilted oval shape that retraces itself.

CP-OCP measurements were performed using a Pt WE to investigate the stability of the OCP when Na^+ is reduced to form alloys with Pt (**Figure 5b**). A current of −0.2 A was applied to the electrochemical system for 10 s immediately after measuring the initial OCP value, resulting in an apparent reduction of Na^+ to Na. Upon measuring the OCP, two distinct plateaus were observed, likely corresponding to the formation of NaPt and $NaPt_2$ alloys. As deposited Na gradually dissolved into the NaCl-KCl molten salt, the composition of the alloy changed, leading to stabilization of the potential over time.

The formation of Na-Pt alloys was also observed during the oxidative scan in the CV, after Na^+ is reduced to Na at an onset reduction potential of approximately −2.2 V for the RE1 $Ni|Ni^{2+}$ (**Figure 5c**). Three oxidative peaks were identified, corresponding from left to right to the oxidation of Na, NaPt, and $NaPt_2$, respectively. All three electrochemical techniques (EIS, CP-OCP, and CV) were performed automatically every hour for over three days to provide insights into the stability of the REs.

3.2.1. EIS Results

The uncompensated resistance for each RE was measured using EIS every hour, starting after the RE had been exposed to the NaCl-KCl molten bath for more than five hours to allow ion permeation through the mullite membrane. Although uncompensated resistance does not directly indicate the stability of the RE, it provides valuable insights into the condition of the molten bath, including its conductivity and the state of the WE. It also provides insights into the resistance of the membrane, as degradation over time would likely result in a gradual increase in resistance. Alternatively, a sudden and significant change in resistance would be expected if the membrane ruptures. The results of the uncompensated resistance measurements for six different REs are shown in **Figure 6**. A deviation of approximately ± 0.04 Ω was observed between the initial and final measurements of solution resistance. This slight deviation could be attributed to minor changes in the conductivity of the molten bath due to impurities over time, slight alterations in the condition or morphology of the WE, or continued ion permeation of the membrane. The conditions for conducting stability tests remain valid as the changes in resistance are small, indicating only minor changes in the system with time.

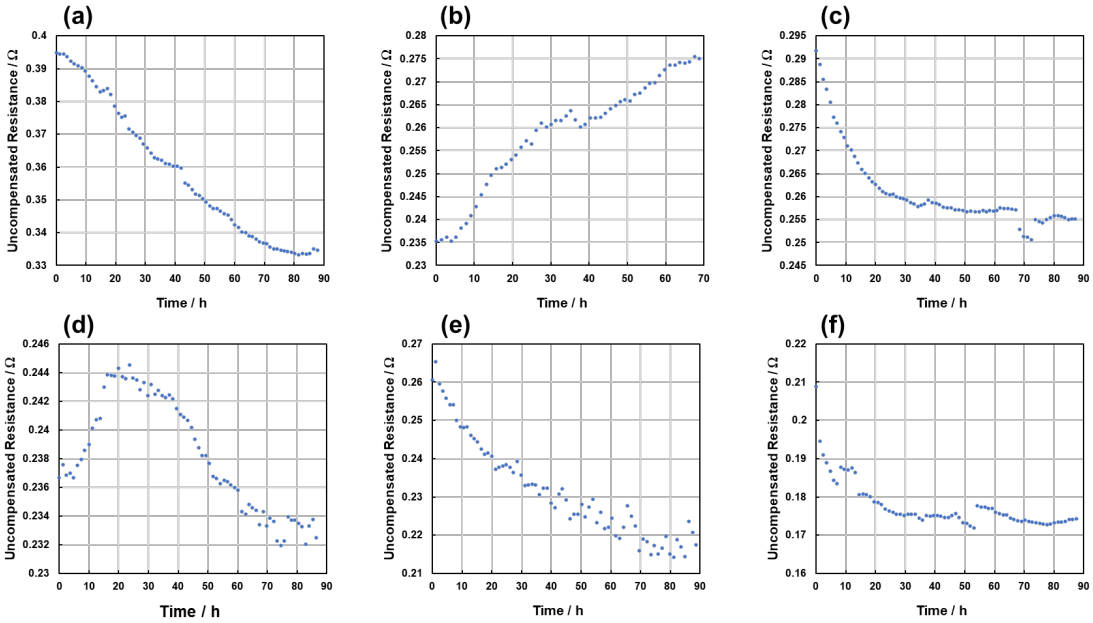

Figure 6. Uncompensated resistance (Z_{re}) obtained through EIS when $-Z_{im}$ is 0 Ω using different REs. **(a)** RE1 Ni|Ni^{2+}, **(b)** RE2 Ni|Ni^{2+}, **(c)** RE3 Ag|Ag^{+}, **(d)** RE4 Ni|Ni^{2+}, **(e)** RE5 NiO|O^{2-}, and **(f)** RE6 NiO|O^{2-}.

3.2.2. OCP Results

The primary parameter for assessing the stability of the RE is the OCP value when Na is deposited on the Pt WE, forming a Na-Pt alloy that provides a stable potential, as shown in our preliminary data. The Na^{+}/Na-Pt couple is expected to have a stable potential due to the abundance of Na^{+} ions in the salt and the constant activity of the Na-Pt alloys. The high concentration of Na^{+} ions places their activity in the flatter region of the logarithmic curve of the Nernst equation, meaning that concentration variations will result in only minor changes to the equilibrium potential.

The procedure for obtaining the OCP value involved taking the average OCP within a time interval where no significant change in potential is observed (i.e., $dE/dt < 10^{-6}$ V s^{-1}), corresponding to the point at which the OCP termination criterion was met. OCP data collected after several runs is presented in **Figure 7**. Each CP run was performed following an EIS measurement and before a CV measurement, with the system allowed to remain idle for one hour before initiating the next run. The OCP usually stabilized within 60 s after CP was applied. However, in some instances, even after the OCP termination criterion was satisfied, the potential continued to drift towards a value like that of a bare Pt WE without metal coating, as observed in Run 70. However, this does not indicate that the RE reached an end-of-life point (i.e., onset of unpredictable behavior), as the OCP curve remained stable after three additional runs, as shown in **Figure S1**. In the case of Run 70, the OCP measurement did not stop, even though the termination criterion had been met. For this specific RE (**Figure 7**), the OCP values for each run were determined by averaging the recorded OCP values between 20 to 60 s. After

each CP-OCP run, the data was exported into a text file, which included a timestamp. Using Python for analysis, the time of the first CP-OCP run was set to 0 h, with subsequent times converted accordingly.

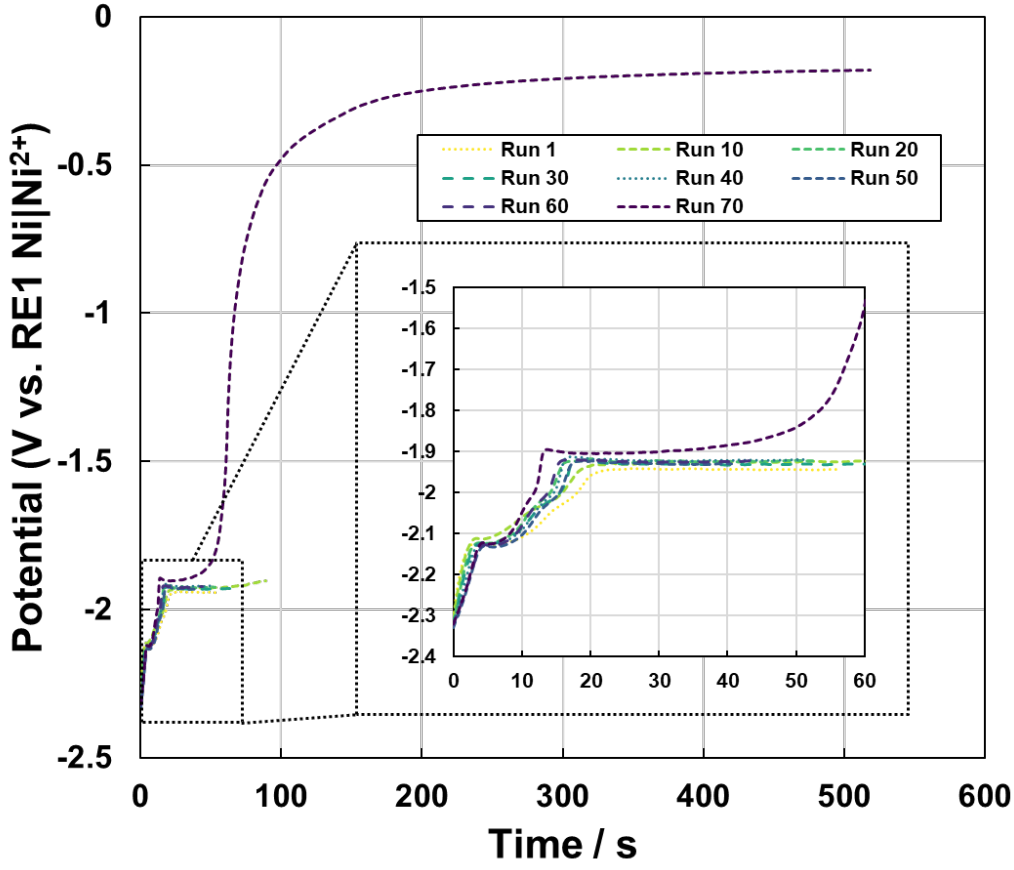

Figure 7. OCP data at 1023 K for the $Na^+/NaPt_2$ redox couple for multiple runs after CP relative to RE1 $Ni|Ni^{2+}$. OCP values, shown in the inset, were averaged in the most stable region between 20 and 60 s, where $dE/dt < 10^{-6}$ V s^{-1}.

Figure 8 shows the results for each RE, displaying OCP values versus time. The time axis represents the time since the first measurement. It does not include the first five hours of exposure to the molten salt to allow for the system to stabilize. Most of the RE demonstrated stable potential over several days; for the REs containing different concentrations of $NiCl_2$, a consistent trend in potential was observed. The OCP values for RE1 $Ni|Ni^{2+}$, RE2 $Ni|Ni^{2+}$, and RE4 $Ni|Ni^{2+}$ were −1.925 V, −2.171 V, and −1.797 V, with standard deviations of 7.8 mV, 9.8 mV, and 8.9 mV, respectively. As shown in **Table 1**, RE1, RE2, and RE4 contained 20, 50, and 4.5 mol%, respectively. Plotting the OCP relative against the natural log of mole fraction resulted in a linear line with a slope of −0.15 ± 0.05 and an intercept of −2.2 ± 0.1 V vs. $Na^+/NaPt_2$. Applying Eq. (1) resulted in an n of 1.7 ± 0.5, where the expected value of 2 is within the standard error of the regression. The potential drift rates for these REs, calculated as the slope of OCP versus time, were 5.0 mV/day, 5.9 mV/day, and 6.6 mV/day for RE1,

RE2, and RE4, respectively. There was a minimal deviation in both potential (average OCP) and standard deviation; however, deviations in potential could be attributed to variations in the uniformity of Na^+ deposition on the Pt WE when forming the Na-Pt alloys. Despite these variations, the REs containing $NiCl_2$ showed minimal OCP deviation, indicating good stability.

The potential of the $Na^+/NaPt_2$ redox couple varied relative to the different REs, suggesting that the analyte concentration plays a crucial role in RE performance. The importance of maintaining a buffered RE with a constant analyte concentration will be discussed later. For comparison, the widely used Ag/AgCl-based RE, represented by RE3 $Ag|Ag^+$, exhibited significant OCP drift relative to the fitted line of OCP versus time, indicating potential instability under certain conditions. The OCP for RE3 $Ag|Ag^+$ was −1.836 V with a standard deviation of 14 mV and a drift of 0.86 mV/day. This drift is not a good representation of the potential drift since it does not follow the trend of the fitted slope, as predicted in **Figure 8c**, making it challenging to assess the potential drift for this RE accurately. In contrast, REs containing NiO showed consistent potentials regardless of analyte concentration. The OCP values for RE5 $NiO|O^{2-}$ and RE6 $NiO|O^{2-}$ were −1.566 V and −1.583 V, with standard deviations of 3.8 mV and 8.3 mV, respectively. Their potential drift rates were 1.2 mV/day for RE5 $NiO|O^{2-}$ and 1.6 mV/day for RE6 $NiO|O^{2-}$. These findings confirm that REs with NiO provided stable and consistent potentials with minimal drift over time. The results comparing different REs are summarized in **Table 2**.

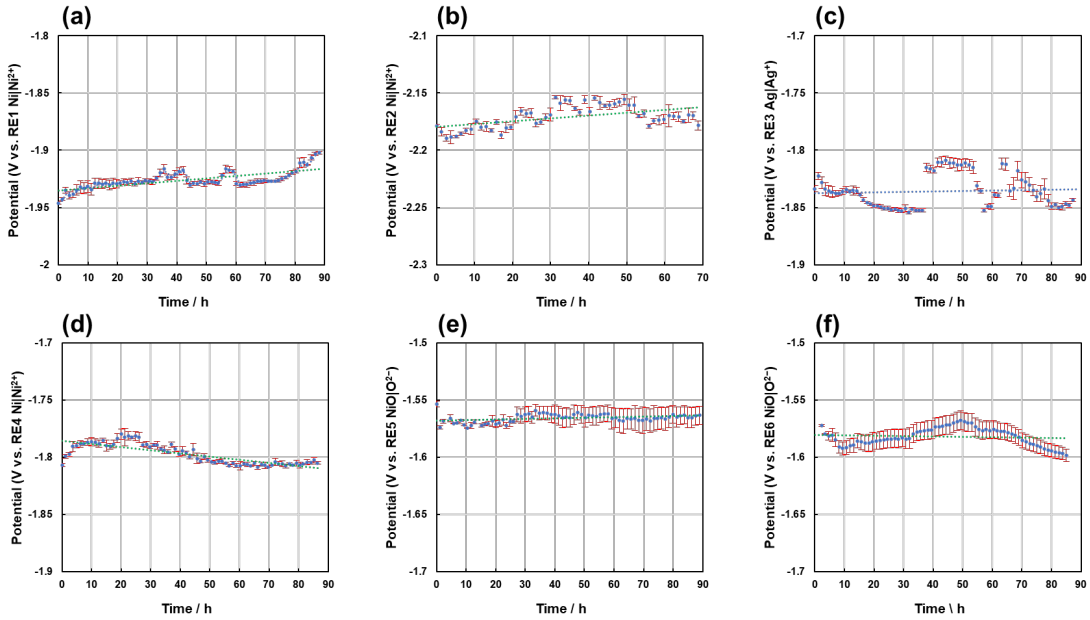

Figure 8. Average OCP values obtained at 1023 K when Na is deposited through CP on Pt WE forming Pt-Na alloys until the potential stabilizes at the $NaPt_2$ plateau within a specific time frame in respect to different REs. **(a)** RE1 $Ni|Ni^{2+}$ (20-60 s), **(b)** RE2 $Ni|Ni^{2+}$ (15-20 s), **(c)** RE3 $Ag|Ag^+$ (10-40 s) **(d)** RE4 $Ni|Ni^{2+}$ (20-30 s), **(e)** RE5 $NiO|O^{2-}$ (20-50 s), and **(f)** RE6 $NiO|O^{2-}$ (20-50 s). Note: OCP time frame was reset to 0 s after CP.

Table 2. Comparison of REs across various analytes and concentrations with their results.

RE	Concentration mol%	Na-Pt Potential (V) [a]	Standard Deviation (mV) [a]	Potential Drift (mV/day) [b]
RE1 $Ni\|Ni^{2+}$	20	−1.925	7.8	5.0
RE2 $Ni\|Ni^{2+}$	50	−2.171	9.8	5.9
RE3 $Ag\|Ag^{+}$	4.5	−1.836	14	0.86
RE4 $Ni\|Ni^{2+}$	4.5	−1.797	8.9	6.6
RE5 $NiO\|O^{2-}$	1.0	−1.566	3.8	1.2
RE6 $NiO\|O^{2-}$	4.5	−1.583	8.3	1.6

[a] Potential determined by averaging all OCP values during stable $NaPt_2$ plateau time range with corresponding standard deviation.

[b] Potential drift determined by taking the absolute slope of the OCP value versus time.

3.2.3. CV Results

Lastly, CV scans were conducted for each RE across 73 different runs, with measurements taken every hour following the CP-OCP measurement (**Figure 9**). The electrochemical window of NaCl-KCl was adjusted according to each RE, as each has its unique redox potential. The CV scans demonstrated a consistent reduction potential for Na, suggesting that the REs maintain stable performance. However, variations in the oxidation peaks were observed across different scans, likely due to variations in deposit morphology and/or thickness of Na and its alloys on the Pt WE, as shown in **Figures 9e** and **9f**. Since all the CV scans consistently overlapped during the onset of the reduction potential over an extended period, this suggests that the REs developed in this study are stable.

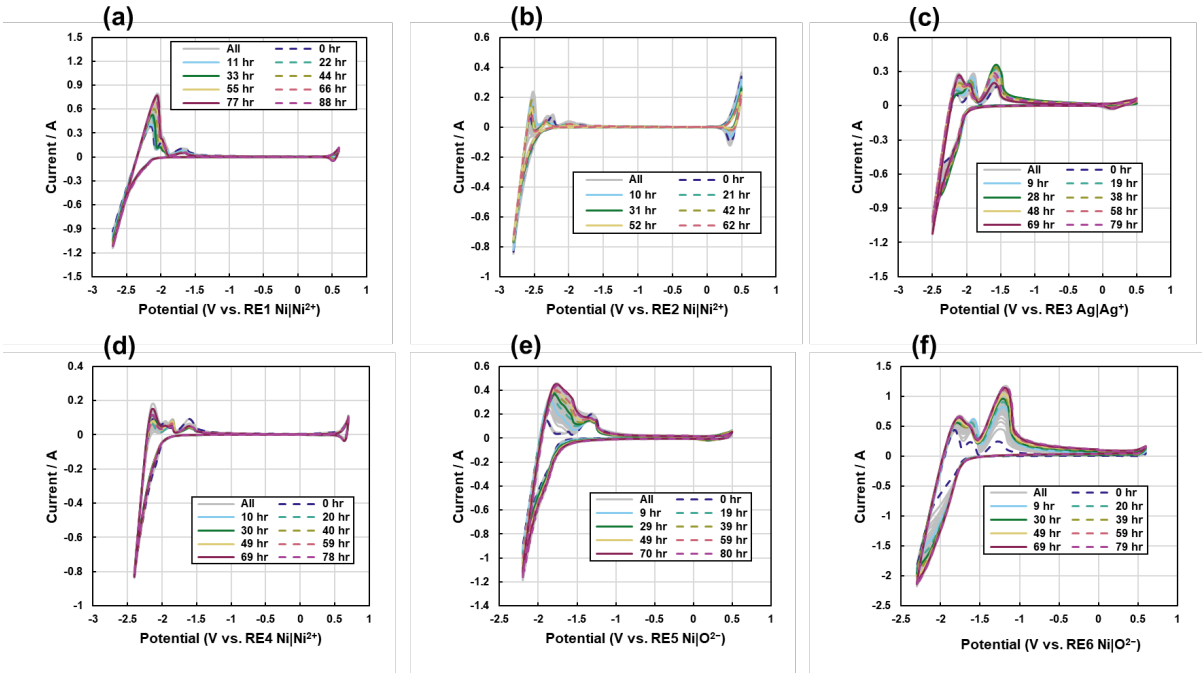

Figure 9. CV scans (fourth scan, 0.1 V s^{-1}) measured within the electrochemical window of equimolar NaCl-KCl at 1023 K over 3-4 days using different REs. **(a)** RE1 Ni|Ni^{2+}, **(b)** RE2 Ni|Ni^{2+}, **(c)** RE3 Ag|Ag^{+}, **(d)** RE4 Ni|Ni^{2+}, **(e)** RE5 NiO|O^{2-}, and **(f)** RE6 NiO|O^{2-}.

3.3. Electrochemical behavior for REs in NaCl-KCl

The electrochemical window of NaCl-KCl was examined using all developed REs with W electrodes to prevent the formation of metal alloys. This investigation aimed to gain a deeper understanding of the redox potential of Na, which could provide valuable insights into the precise lower limit of electrorefining of metals, thereby minimizing the reduction of impurities during pyrochemical processing. The electrochemical window, illustrated in **Figure 10**, was assessed following the completion of stability tests for each RE. It was observed that the electrochemical window shifted for REs containing $NiCl_2$ and AgCl, which is consistent with the OCP data, where variations in potential were noted for different analyte concentrations. Conversely, regardless of concentration, the electrochemical window for REs containing NiO remained relatively constant. The underlying reasons for this behavior will be elaborated on in the subsequent subsection.

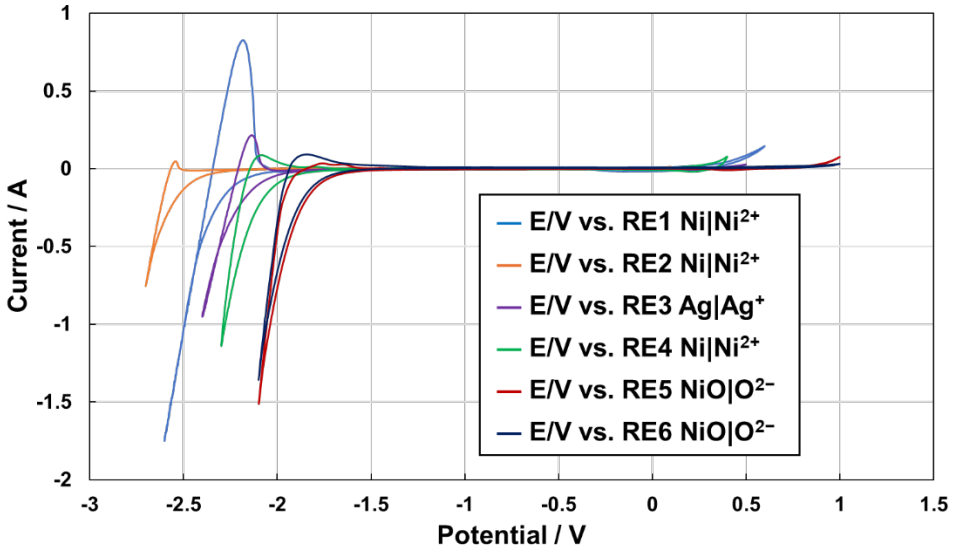

Figure 10. Full electrochemical window of equimolar NaCl-KCl at 1023 K using different REs. WE: 1.5 mm W rod. CE: 3.175 mm W rod. Scan rate: 0.1 V s^{-1}.

3.3.1. Metal chloride REs

Developing a stable and buffered RE is essential for electrorefining and electrowinning, as fluctuations in cathode potential compromise the purity of the desired metal. The Nernst equation and the corresponding redox couple determine the redox potential of a RE. Ag/AgCl-based REs are widely utilized in molten salt applications, and their stability with various membranes and concentrations has been extensively studied, as discussed in Introduction (Section 1). However, any minor variation in the activity of the analyte ion, Ag^+, can influence the redox potential, especially at low concentrations, as demonstrated by the following expression:

$$E = E^{o\prime}_{Ag/Ag^+} - \frac{RT}{nF} ln(\alpha_{Ag^+}) = E^{o\prime}_{Ag/Ag^+} - \frac{RT}{nF} ln\left(\frac{C_{Ag^+}}{C^o}\right), \quad (2)$$

where $\alpha_{Ag^+} = \gamma_{Ag^+} \cdot C_{Ag^+}/C^o$. Here, γ_{Ag^+} represents the activity coefficient of Ag^+, $E^{o\prime}$ is the formal potential, C^o is the standard concentration, usually 1 M or 1 m, and C_{Ag^+} denotes the mole fraction of Ag^+. Assuming ideal behavior in dilute systems, the activity coefficient can be approximated as one, implying that the activity of Ag^+ is directly related to their concentration. Due to the relatively low melting point of AgCl (728 K), creating a saturated phase (i.e., a solid-liquid equilibrium) is challenging. Consequently, the potential can vary with changes in Ag^+ concentration. Furthermore, the evaporation of AgCl can alter the potential over time. However, in our study, this effect was minimized by the enclosure of the analyte within the membrane, which effectively reduced evaporation.

$NiCl_2$ was chosen as the analyte for developing a buffered and stable RE due to its high melting point (1274 K) and potential to form a secondary phase, as reported in single chloride molten salts [48,49]. However, limited research exists on the ternary phase diagram of NaCl-KCl-$NiCl_2$, making it challenging to determine the minimum $NiCl_2$ concentration required to form a secondary phase. Thermochemical simulations using FactSage 8.2 were employed to model the phase behavior of this ternary chloride system [50]. According to the simulated phase diagram (**Figure S2**), a minimum of 50 mol% $NiCl_2$ is required to form a secondary phase at the operating temperature of 1023 K in an equimolar NaCl-KCl molten salt.

$NiCl_2$ was incrementally added to NaCl-KCl in a quartz tube (TTL95, Technical Glass Products, Inc.) and heated until molten to validate the simulation results experimentally. A notable thermochromic transition was observed upon cooling to room temperature, with the color changing from dark red in the molten state to blue, suggesting peritectic $KNiCl_3$ and eventually to orange upon solidification (**Figure S3**) [51]. This color change may influence the redox potential across different temperatures, which requires further investigation.

The saturation point of $NiCl_2$ was evaluated by observing precipitate formation upon cooling. Small precipitates appeared when the $NiCl_2$ concentration reached 7.03 mol% (**Figure S4-b**), although they were not visible in the molten state. More pronounced precipitates formed at higher concentrations (i.e., > 17.75 mol%), although these were still difficult to detect while molten. We were unable to dismiss the possibility that the precipitate formation occurs primarily upon solidification and does not necessarily indicate secondary phase formation in the molten state.

Increasing $NiCl_2$ concentrations further was constrained by its sublimation behavior, as evidenced by TGA (Netzsch, STA 449 F5 Jupiter) data (**Figure S5-a**), which showed significant sublimation beginning at 1063 K (790 °C). Electrochemical measurements using a two-electrode system, with a bismuth-nickel (Bi-Ni) alloy consisting of 30 mol% Ni and 70 mol% Bi, as the WE, indicated the OCP values rose beyond 10 mol% $NiCl_2$ (**Figure S5-b**). This observation contradicts the visual experiments, where precipitates were observed with 7.03 mol% $NiCl_2$ (**Figure S4-b**) upon solidification, suggesting that the secondary phase was not achieved in the molten state.

While thermodynamic simulations predict that at least 50 mol% $NiCl_2$ is required to form a saturated secondary phase, experimental results indicate that achieving this phase without complications is challenging. High concentrations of $NiCl_2$ introduce complexities, such as non-ideal activity coefficients and large junction potentials, which could undermine the stability and functionality of saturated REs. Thus, further investigation of $NiCl_2$ behavior is necessary to optimize RE performance while minimizing potential issues.

3.3.2. Metal oxide REs

To better understand the electrochemical behavior of NaCl-KCl when NiO is used as the analyte in the RE, we investigated the electrochemical window of NaCl-KCl using a RE made of Ni wire encased in a mullite tube containing NaCl-KCl without any analyte. The results revealed differences in the electrochemical window between the RE containing NiO and the RE without analyte (**Figure 11**). Previous reports indicate that the solubility of NiO in NaCl-KCl is at the ppm level, leading us to explore using NiO as an analyte to deliver a saturated and buffered RE [52]. Regardless of the concentration, the solubility limit ensures a consistent dissolution of Ni^{2+} and O^{2-} ions when NiO dissolves in molten NaCl-KCl.

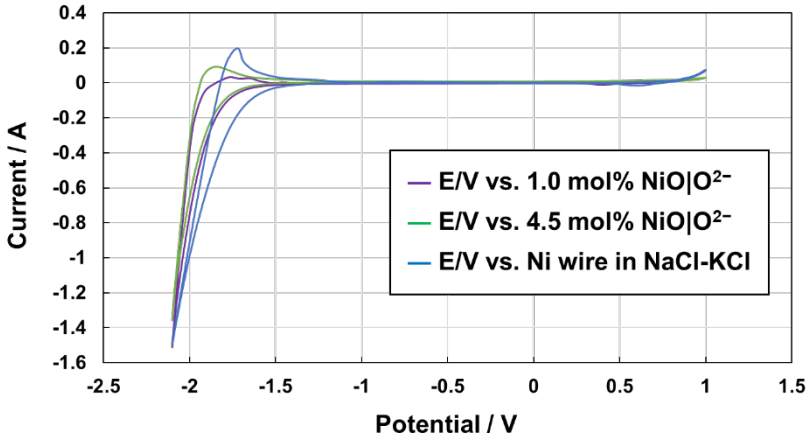

Figure 11. Full electrochemical window of equimolar NaCl-KCl at 1023 K using different REs. WE: 1.5 mm W rod. CE: 3.175 mm W rod. Scan rate: 0.1 V s^{-1}.

The Nernst equation for the redox reaction is based on the activities of Ni and O^{2-}, with the activity of the metal assumed to be one. Consequently, the potential of the NiO RE depends predominately on the activity of O^{2-}. Given that the solubility of NiO is in the ppm range, we assume that the activity of NiO is constant at a given temperature either due to its saturation in the molten salt or its presence as a solid film on the Ni wire with excess NiO precipitate in the bottom of the mullite tube. Hence, the activity of NiO is taken as one or included in the formal potential ($E^{o\prime}_{NiO/O^{2-}}$). Therefore, the potential is primarily determined by the concentration of O^{2-}, as expressed based on the following reaction:

$$NiO_s + 2e^- \rightleftharpoons \mathrm{Ni}_s + \mathrm{O}^{2-}_{sln}\,, \tag{3}$$

which results in the following equation for the equilibrium potential:

$$E = E^{o\prime}_{NiO/O^{2-}} - \frac{RT}{nF} ln\left(\frac{\alpha_{Ni}\cdot\alpha_{O^{2-}}}{\alpha_{NiO}}\right) = E^{o\prime}_{NiO/O^{2-}} - \frac{RT}{2F} ln(\alpha_{O^{2-}}) = E^{o\prime}_{NiO/O^{2-}} - \frac{RT}{2F} ln\left(\frac{C_{O^{2-}}}{C^o}\right). \tag{4}$$

The electrochemical window measurements of NaCl-KCl suggest that the O^{2-} concentration remains constant in REs containing 1.0 mol% and 4.5 mol% NiO, indicating that we successfully fabricated a saturated and stable RE independent of NiO concentration. The O^{2-} concentration in the RE was determined by back titration, which showed that the oxygen content in NaCl-KCl without NiO was 2.624 ppm, while the oxygen content in NaCl-KCl containing NiO was 43.125 ppm by weight, which is consistent with solubility of NiO reported in the literature [52,53]. This finding supports the idea that the oxygen content remains stable due to the low solubility limit of NiO, making it an ideal approach for consistent RE fabrication.

This study demonstrates that NiO-based REs can provide reliable performance across various molten salts by creating a saturated solution buffered by the excess NiO. They offer a promising method for ensuring consistency in processes like electrorefining, where the purity of refined metals is critical, or when reporting potentials relative to chlorine ion-chlorine gas redox couple (Cl^-/Cl_2). These findings lay the groundwork for the broader application of metal oxide-based saturated and buffered REs in future electrochemical systems.

4. Conclusions

This study investigated the stability of REs containing various analytes when exposed to NaCl-KCl molten salts over extended periods. REs containing metal chlorides and oxides demonstrated stability over time; however, REs containing AgCl exhibited more significant fluctuations in potential. The potential of REs containing metal chlorides varied at different concentrations, preventing their use as buffered REs. The behavior of $NiCl_2$ in NaCl-KCl was explored to identify its saturation point and the formation of a secondary phase through OCP measurements and visual inspection. A stable OCP indicating saturation was not observed beyond 10 mol% $NiCl_2$, suggesting that higher concentrations are necessary to achieve saturation. This finding aligns with the simulated ternary phase diagram, which predicted that a minimum of 50 mol% $NiCl_2$ is required to form a secondary phase. However, the high concentration of $NiCl_2$ can lead to large junction potentials, making it impractical for RE applications.

In contrast, REs based on metal oxides demonstrated both stability and a buffered potential across a wide range of concentrations due to the low solubility of NiO in NaCl-KCl, which remains at ppm levels. As a result, the oxide concentration in the REs remains effectively constant, providing ideal conditions as predicted by the Nernst equation, where the concentration of oxidized species determines the potential. The electrochemical window of NaCl-KCl was consistent across the fabricated metal oxide REs, and the oxygen content was quantified via back titration.

Our findings indicate that metal oxide-based REs offer superior stability and reliability for use in pyrochemical processes, such as electrorefining, where monitoring a stable potential is critical to maintaining the purity of the refined metal. The development of such stable and buffered REs ensures that

secondary species are not reduced into the metal, making them highly advantageous for industrial applications with high production demands.

Author contributions

C.M. and D.R. conceived and designed the experiment. D.R. supervised the project. C.M. fabricated the REs, prepared the molten salts, performed the electrochemical measurements and back titration, and analyzed the data. N.C. assisted with the preparation of salts and the visual representations of the molten salts. R.R.C. prepared the salts for the back titration measurements. C.M. and D.R. prepared the manuscript with contributions from all authors. All authors have approved the final version of the manuscript.

Conflicts of interest

The authors declare that they have no known competing financial interests or personal relationships that could have appeared to influence the work reported in this paper.

Acknowledgments

We gratefully acknowledge funding for this work from the U.S. Department of Energy, NNSA, Plutonium Maturation Program (NA-191) in collaboration with Los Alamos National Laboratory.

References

[1] O. Takeda, M. Li, T. Toma, K. Sugiyama, M. Hoshi, Y. Sato, Electrowinning of Lithium from LiOH in Molten Chloride, J. Electrochem. Soc. 161 (2014) D820–D823. https://doi.org/10.1149/2.0871414jes.

[2] G.M. Haarberg, Electrowinning of Light Metals from Molten Salts Electrolytes, ECS Trans. 114 (2024) 13–21. https://doi.org/10.1149/11406.0013ecst.

[3] E. Aghion, G. Golub, Production Technologies of Magnesium, in: H.E. Friedrich, B.L. Mordike (Eds.), Magnes. Technol. Metall. Des. Data Appl., Springer, Berlin, Heidelberg, 2006: pp. 29–62. https://doi.org/10.1007/3-540-30812-1_2.

[4] Y. Sakamura, T. Hijikata, K. Kinoshita, T. Inoue, T.S. Storvick, C.L. Krueger, L.F. Grantham, S.P. Fusselman, D.L. Grimmett, J.J. Roy, Separation of Actinides from Rare Earth Elements by Electrorefining in LiC1-KC1 Eutectic Salt, J. Nucl. Sci. Technol. 35 (1998) 49–59. https://doi.org/10.1080/18811248.1998.9733819.

[5] K. Kinoshita, T. Koyama, T. Inoue, M. Ougier, J.-P. Glatz, Separation of actinides from rare earth elements by means of molten salt electrorefining with anodic dissolution of U–Pu–Zr alloy fuel, J. Phys. Chem. Solids 66 (2005) 619–624. https://doi.org/10.1016/j.jpcs.2004.06.069.

[6] S. Delpech, Molten Salts for Nuclear Applications, in: Molten Salts Chem., Elsevier, 2013: pp. 497–520. https://doi.org/10.1016/B978-0-12-398538-5.00024-X.

[7] R. Roper, M. Harkema, P. Sabharwall, C. Riddle, B. Chisholm, B. Day, P. Marotta, Molten salt for advanced energy applications: A review, Ann. Nucl. Energy 169 (2022) 108924. https://doi.org/10.1016/j.anucene.2021.108924.

[8] T. Williams, R. Shum, D. Rappleye, Concentration Measurements In Molten Chloride Salts Using Electrochemical Methods, J. Electrochem. Soc. 168 (2021) 123510. https://doi.org/10.1149/1945-7111/ac436a.

[9] W. Yang, R.I. Foster, J. Kim, S. Choi, Electrochemical Monitoring for Molten Salt Pyroprocessing of Spent Nuclear Fuel: A Review, Korean J. Chem. Eng. 41 (2024) 2781–2797. https://doi.org/10.1007/s11814-024-00260-9.

[10] N.K. Al-Shara, F. Sher, A. Yaqoob, G.Z. Chen, Electrochemical investigation of novel reference electrode Ni/Ni(OH)$_2$ in comparison with silver and platinum inert quasi-reference electrodes for electrolysis in eutectic molten hydroxide, Int. J. Hydrog. Energy 44 (2019) 27224–27236. https://doi.org/10.1016/j.ijhydene.2019.08.248.
[11] D. Rappleye, K. Teaford, M. Simpson, Investigation of the Effects of Uranium(III)-Chloride Concentration on Voltammetry in Molten LiCl-KCl Eutectic with a Glass-Tungsten Fused Electrode, Electrochimica Acta 219 (2016) 721–733. https://doi.org/10.1016/j.electacta.2016.10.075.
[12] B.K.K. Kasem, S. Jones, Platinum as a Reference Electrode in Electrochemical Measurements, Platin. Met. Rev. 52 (2008) 100–106. https://doi.org/10.1595/147106708X297855.
[13] L. Martinot, F. Caligara, Electrochemistry of actinides in molten salts, At. Energy Rev. 11 (1973) 3–61.
[14] D. Killinger, S. Phongikaroon, Investigation of W, Ag, and Pt Quasi-Reference Electrode Stability in Molten NaCl-CaCl $_2$ with Ce(0)/Ce(III) as an Internal Reference Redox Reaction, J. Electrochem. Soc. 168 (2021) 036518. https://doi.org/10.1149/1945-7111/abef4a.
[15] C. Sun, Q. Xu, X. Zou, H. Cheng, X. Lu, A new method to determine AgCl(1% mol)/Ag electrode potential versus the standard chloride electrode potential in a LiCl-KCl eutectic, Electrochem. Commun. 130 (2021) 107111. https://doi.org/10.1016/j.elecom.2021.107111.
[16] R. Littlewood, A reference electrode for electrochemical studies in fused alkali chlorides at high temperatures, Electrochimica Acta 3 (1961) 270–278. https://doi.org/10.1016/0013-4686(61)85003-2.
[17] R. Pal, K. Ananthasivan, S. Anthonysamy, V. Ganesan, Development and electrochemistry of a novel Ag/AgCl reference electrode suitable for mixed chloride–fluoride melts, Electrochimica Acta 56 (2011) 4276–4280. https://doi.org/10.1016/j.electacta.2011.01.080.
[18] K. Yasuda, T. Nohira, Y.H. Ogata, Y. Ito, Electrochemical window of molten LiCl–KCl–CaCl2 and the Ag+/Ag reference electrode, Electrochimica Acta 51 (2005) 561–565. https://doi.org/10.1016/j.electacta.2005.05.014.
[19] D. Yoon, A. Baggett, S. Phongikaroon, J.A. King, K. Marsden, Fundamental Data Acquisition toward Silver-Silver Chloride Reference Electrode, J. Electrochem. Soc. 166 (2019) E159. https://doi.org/10.1149/2.0721906jes.
[20] J. Song, X. Huang, Y. Fan, J. Yi, Y. Shu, J. He, In Situ Monitoring of O2− Concentration in Molten NaCl-KCl at 750°C, J. Electrochem. Soc. 165 (2018) E245. https://doi.org/10.1149/2.1101805jes.
[21] G.W. Harrington, H.T. Tien, A REFERENCE ELECTRODE FOR CERTAIN MOLTEN SALT SOLUTIONS, J. Phys. Chem. 66 (1962) 173–174. https://doi.org/10.1021/j100807a501.
[22] C.R. Lhermitte, S.S. Parker, J.M. Jackson, M.J. Monreal, Communication—Mg2+/0 as a Reliable Reference Electrode for Molten Chloride Salts, J. Electrochem. Soc. 168 (2021) 066501. https://doi.org/10.1149/1945-7111/ac0303.
[23] P. Bagri, M.F. Simpson, Activity Measurements of Gadolinium(III) Chloride in Molten LiCl-KCl Eutectic Salt Using Saturated Gd/GdCl3 Reference Electrode, J. Electrochem. Soc. 164 (2017) H5299. https://doi.org/10.1149/2.0441708jes.
[24] M. Newton, T. Meaders, J. Steppan, S. Bae, M. Simpson, Stability of a Ni/NiF $_2$ Reference Electrode with a Metallic Membrane for Use in Molten Fluoride Salts, J. Electrochem. Soc. 171 (2024) 077509. https://doi.org/10.1149/1945-7111/ad5cc3.
[25] S. Yoon, D. Kang, S. Sohn, J. Park, M. Lee, S. Choi, Reference Electrode at Molten Salt: A Comparative Analysis of Electroceramic Membranes, J. Nucl. Fuel Cycle Waste Technol. 18 (2020) 143–155. https://doi.org/10.7733/jnfcwt.2020.18.2.143.
[26] H. Wang, N.J. Siambun, L. Yu, G.Z. Chen, A Robust Alumina Membrane Reference Electrode for High Temperature Molten Salts, J. Electrochem. Soc. 159 (2012) H740–H746. https://doi.org/10.1149/2.033209jes.
[27] D.-D. Wang, Y.-L. Liu, Y.-K. Zhong, S.-L. Jiang, W. Han, L. Wang, W.-Q. Shi, Long-life mullite and boron nitride membranes Ag/AgCl and Pb/PbCl2 reference electrodes for LiCl-KCl eutectic melt, J. Electroanal. Chem. 952 (2024) 117949. https://doi.org/10.1016/j.jelechem.2023.117949.
[28] S. Choi, J. Steppan, M.F. Simpson, Long-Term Stability of Mullite and Magnesia-encased Ag|Ag+ Reference Electrodes in Molten MgCl2-KCl-NaCl, J. Electrochem. Soc. 170 (2023) 057505. https://doi.org/10.1149/1945-7111/acd35a.

[29] P. Gao, X. Jin, D. Wang, X. Hu, G.Z. Chen, A quartz sealed Ag/AgCl reference electrode for CaCl2 based molten salts, J. Electroanal. Chem. 579 (2005) 321–328. https://doi.org/10.1016/j.jelechem.2005.03.004.
[30] J. Kruger, K.H. Stern, Surface Behavior of Silver Single Crystals in Fused Sodium Chloride, J. Electrochem. Soc. 109 (1962) 889. https://doi.org/10.1149/1.2425202.
[31] D. Rappleye, J. McNeese, R. Torres, K. Holliday, J.R. Jeffries, Development of small-scale plutonium electrorefining in molten CaCl2, J. Nucl. Mater. 552 (2021) 152968. https://doi.org/10.1016/j.jnucmat.2021.152968.
[32] M. Mirza, R. Abdulaziz, W. C. Maskell, S. Wilcock, A. H. Jones, S. Woodall, A. Jackson, P. R. Shearing, D.J. L. Brett, Electrochemical processing in molten salts – a nuclear perspective, Energy Environ. Sci. 16 (2023) 952–982. https://doi.org/10.1039/D2EE02010F.
[33] G. Bourges, G. Bourgès, D. Lambertin, D. Lambertin, S. Rochefort, S. Delpech, G. Picard, Electrochemical studies on plutonium in molten salts, J. Alloys Compd. 444 (2007) 404–409. https://doi.org/10.1016/j.jallcom.2006.10.095.
[34] Y.-H. Jia, H. He, R.-H. Lin, H.-B. Tang, Y.-Q. Wang, Electrochemical behavior of cerium(III) in NaCl–KCl molten salt, J. Radioanal. Nucl. Chem. (2014). https://doi.org/10.1007/s10967-014-3723-8.
[35] G. Chipman, B. Johnson, C. Vann, L. Whitesides, D. Rappleye, Experimental determination of the electrochemical properties of bismuth chloride in eutectic LiCl–KCl and LiCl–KCl–CaCl2 molten salts, J. Radioanal. Nucl. Chem. (2024). https://doi.org/10.1007/s10967-024-09354-4.
[36] D. Lambertin, S. Ched'homme, G. Bourgès, S. Sanchez, G. Picard, Plutonium chemical properties in NaCl–KCl and CaCl2 at 1073K, J. Nucl. Mater. 341 (2005) 124–130. https://doi.org/10.1016/j.jnucmat.2005.01.010.
[37] J.J. Roy, L.F. Grantham, D.L. Grimmett, S.P. Fusselman, C.L. Krueger, T.S. Storvick, T. Inoue, Y. Sakamura, N. Takahashi, Thermodynamic Properties of U, Np, Pu, and Am in Molten LiCl-KCl Eutectic and Liquid Cadmium, J. Electrochem. Soc. 143 (1996) 2487. https://doi.org/10.1149/1.1837035.
[38] O. Shirai, T. Iwai, Y. Suzuki, Y. Sakamura, H. Tanaka, Electrochemical behavior of actinide ions in LiCl-KCl eutectic melts., J. Alloys Compd. 271–273 (1998) 685–688. https://doi.org/10.1016/S0925-8388(98)00187-X.
[39] J. Serp, R.J.M. Konings, Rudy J. M. Konings, R.J.M. Konings, R. Malmbeck, J. Rebizant, C. Scheppler, J.-P. Glatz, Electrochemical behaviour of plutonium ion in LiCl–KCl eutectic melts, J. Electroanal. Chem. 561 (2004) 143–148. https://doi.org/10.1016/j.jelechem.2003.07.027.
[40] J.M. Torrie, R. Fuller, D. Rappleye, Communication—The Development of a Stable and Practical Saturated Reference Electrode for Molten Chloride Salt Systems, J. Electrochem. Soc. 171 (2024) 053508. https://doi.org/10.1149/1945-7111/ad4c0c.
[41] D. Chen, K. Du, W. Li, P. Wang, L. Guo, B. Deng, W. Li, H. Yin, D. Wang, A Highly Reliable Ni/NiO Reference Electrode for Molten Li-Na-K Carbonates, J. Electrochem. Soc. 169 (2022) 106519. https://doi.org/10.1149/1945-7111/ac93bb.
[42] O.R. Dale, F. Felling, M. Gonzalez, C. Zhang, M.F. Simpson, Ni/NiO Reference Electrode Potential Measurements in Molten $CaCl_2$–CaO, J. Electrochem. Soc. 170 (2023) 066509. https://doi.org/10.1149/1945-7111/acdd25.
[43] A.J. Burak, M.F. Simpson, Electrochemical Measurement of Li2O in Molten LiCl Salt, ECS Trans. 75 (2016) 55. https://doi.org/10.1149/07515.0055ecst.
[44] A.N. Williams, G. Cao, M.R. Shaltry, Voltammetry measurements in lithium chloride-lithium oxide (LiCl–Li2O) salt: An evaluation of working electrode materials, J. Nucl. Mater. 546 (2021) 152760. https://doi.org/10.1016/j.jnucmat.2020.152760.
[45] W. Zhang, C.R. Pulham, A.R. Mount, N. Brockie, R. Lewin, Thermodynamic calculation and reference electrode calibration for high temperature molten salts, Energy Mater. 3 (2008) 132–136. https://doi.org/10.1179/174892408X394254.
[46] G. Durán-Klie, D. Rodrigues, S. Delpech, Dynamic Reference Electrode development for redox potential measurements in fluoride molten salt at high temperature, Electrochimica Acta 195 (2016) 19–26. https://doi.org/10.1016/j.electacta.2016.02.042.
[47] M. Zhang, J. Ge, J. Zhang, L.E. Liu, Redox potential measurement of AgCl in molten LiCl-KCl

salt using chronopotentiometry and potentiodynamic scan techniques, Electrochem. Commun. 105 (2019) 106498. https://doi.org/10.1016/j.elecom.2019.106498.
[48] The American Ceramic Society and the National Institute of Standards and Technology, Phase Equilibria Diagrams Online Database (NIST Standard Reference Database 31), Fig. Numbers 1309 3103 17652-D (2024). https://www.nist.gov/srd/nist-standard-reference-database-31.
[49] C. Robelin, P. Chartrand, A.D. Pelton, Thermodynamic evaluation and optimization of the (NaCl + KCl + MgCl2 + CaCl2 + MnCl2 + FeCl2 + CoCl2 + NiCl2) system, J. Chem. Thermodyn. 36 (2004) 809–828. https://doi.org/10.1016/j.jct.2004.05.005.
[50] C.W. Bale, E. Bélisle, P. Chartrand, S.A. Decterov, G. Eriksson, A.E. Gheribi, K. Hack, I.-H. Jung, Y.-B. Kang, J. Melançon, A.D. Pelton, S. Petersen, C. Robelin, J. Sangster, P. Spencer, M.-A. Van Ende, FactSage thermochemical software and databases, 2010–2016, Calphad 54 (2016) 35–53. https://doi.org/10.1016/j.calphad.2016.05.002.
[51] D. Visser, G.C. Verschoor, D.J.W. Ijdo, The structure of KNiCl3 at room temperature, Acta Crystallogr. B 36 (1980) 28–34.
[52] T. Ishitsuka, K. Nose, Stability of protective oxide films in waste incineration environment—solubility measurement of oxides in molten chlorides, Corros. Sci. 44 (2002) 247–263. https://doi.org/10.1016/S0010-938X(01)00059-2.
[53] R.A. Sheikh, The synthesis of cementitious compounds in molten salts, University College London, 2016. https://discovery.ucl.ac.uk/id/eprint/1474690/.

Supporting Information

Development of a Stable and Buffered Reference Electrode for Binary Molten Chlorides Salts

Carlos Mejia[1,], Nicholas Christensen[1], Ricardo Rodriguez Ceron[1], and Devin Rappleye[1]*

[1] Department of Chemical Engineering, Brigham Young University, Provo, Utah 84602 USA

* Corresponding author: carlos_mejia@byu.edu

This file includes:

Text S1. Additional information for the last four runs in CP measurements that indicate a lack of end-of-life behavior for RE1 Ni|Ni^{2+}.

The stability test of the developed reference electrodes (REs) was conducted by applying a small current (−0.2 A) to the Pt WE to reduce Na metal on its surface, forming a stable Na-Pt alloy. The OCP was then characterized after the CP, with the results of the last four runs shown in **Figure S1**. In the main manuscript, only Run 70 was presented, which could lead to confusion as it might be interpreted as indicating an end-of-life run.

The Nova 2.1.7 software was programmed to stop OCP measurements and proceed to the next electrochemical measurement, CV, when the condition $dE/dt < 10^{-6}$ V s^{-1} for ten identical OCP values measured every 0.1 s were observed. However, in some cases, even when these conditions were met, the software failed to recognize them, resulting in the OCP measurement continuing until no stable OCP value could be observed. As a result, the alloy stripped back into the solution, causing the potential to eventually return to the OCP value of the Pt WE itself, corresponding to the redox potential of the salt or small impurities. Notably, for Runs 71 and 72, which followed Run 70, the conditions for a stable OCP were successfully met, and a stable potential was obtained.

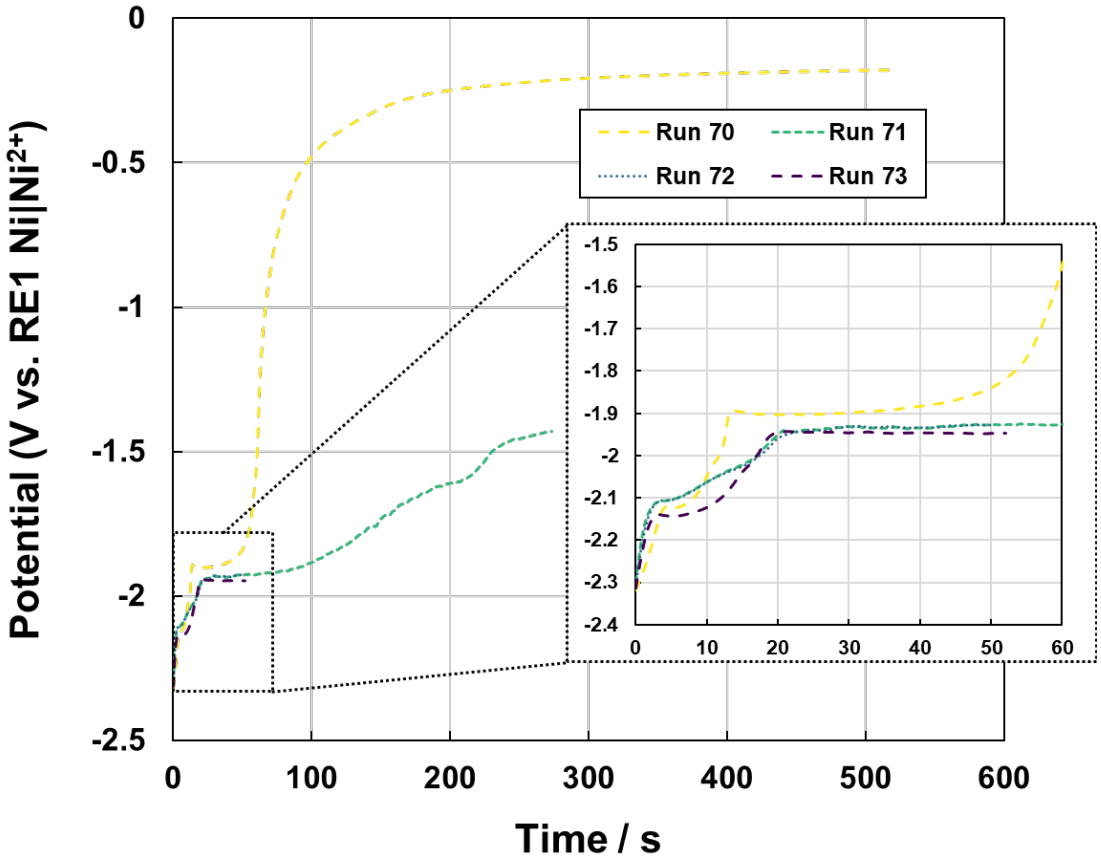

Figure S1. OCP data for the last four runs after CP for RE1 Ni|Ni^{2+}. OCP values, as shown in the inset, obtained by averaging the stable OCP measurements recorded between 20 and 60 s.

Text S2. Thermodynamics simulations for the ternary phase diagram of NaCl-KCl-$NiCl_2$ using FactSage 8.2.

A study reported the ternary phase diagram of the NaCl-KCl-$NiCl_2$ system [1], which is critical for developing a buffered and saturated reference electrode (SRE). Here, we simulated the ternary phase diagram using FactSage 8.2, utilizing available thermodynamic data for NaCl, KCl, and $NiCl_2$. The simulated phase diagram was set to temperatures from 773 K (500 °C) to 1273 K (1000 °C), and the resulting phase diagram is presented in **Figure S2**. The simulated results agree well with the previously reported results, which report a liquidus temperature of 1023 K (750 °C) in the vicinity of 50 mol% of $NiCl_2$ [1].

The ternary phase diagram analysis reveals a peritectic point for $KNiCl_3$ when the molten salt composition includes an equimolar mixture of NaCl-KCl and 30 mol% $NiCl_2$ at 823 K (550 °C). The minimum $NiCl_2$ concentration required to form a liquid-solid phase in equimolar NaCl-KCl is 50 mol% at an operational temperature of 1023 K (750 °C). However, this high composition poses challenges for use in a RE, as it can induce junction potentials or dendritic growth within the RE wire. Therefore, a composition below 50 mol% $NiCl_2$ is preferred to minimize these issues, restricting the ability to maintain a SRE. The slight deviations in $NiCl_2$ concentration could lead to potential drift, impacting RE stability.

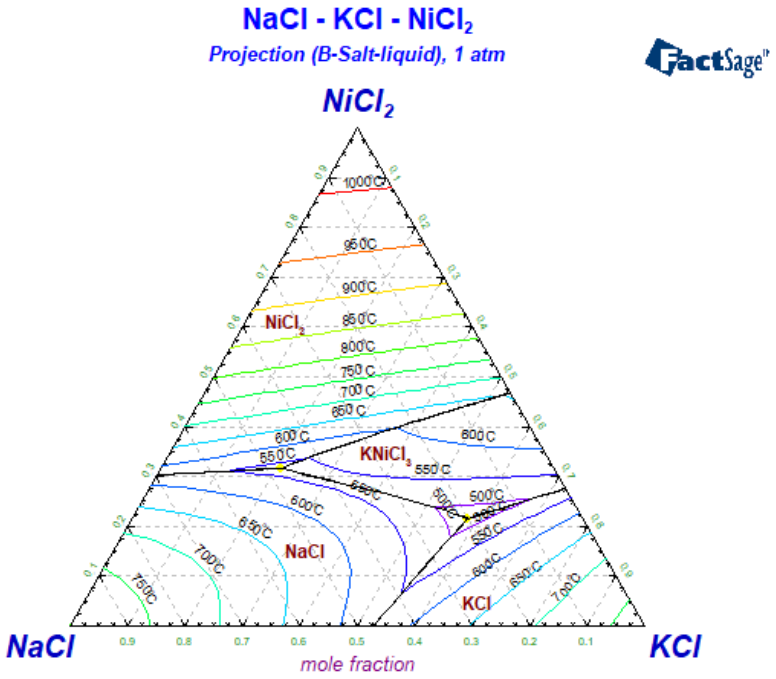

Figure S2. Ternary phase diagram of NaCl-KCl-$NiCl_2$ obtained using FactSage 8.2.

Text S3. Experimental observations on the effect of $NiCl_2$ in equimolar NaCl-KCl molten salts and investigation of $NiCl_2$ saturation point.

An experiment was conducted in which 0.5 mol% $NiCl_2$ was added to equimolar NaCl-KCl within a quartz tube. The mixture was heated to 1073 K in a muffle furnace to melt the salt, then rapidly removed to observe its solidification behavior as it cooled to room temperature (**Figure S3**). The addition of $NiCl_2$ caused the molten salt to turn to a red-orange color, which transitioned to blue in the liquid phase upon cooling. This suggests the peritectic $KNiCl_3$ formation, as predicted by the simulated phase diagram, and then changed to orange upon solidification. This thermochromic effect induced by $NiCl_2$

highlights potential challenges in using it as an analyte in a RE, especially under variable temperature conditions in molten salts.

The saturation point of $NiCl_2$ in NaCl-KCl was assessed through visual and electrochemical methods (**Figures S4** and **S5b**). Incremental additions of $NiCl_2$, ranging from 3.90 mol% to 30.04 mol%, were incorporated into the NaCl-KCl melt until a visible $NiCl_2$ precipitate could appear. While no precipitates were observed in the molten state, cooling to room temperature revealed small $NiCl_2$ precipitates at a concentration of 7.03 mol% (**Figure S4b**). Open-circuit potential (OCP) measurements were taken after each $NiCl_2$ addition in a two-electrode setup. The working electrode (WE), submerged in an inner crucible containing Ni-Bi molten metal, and the tungsten (W) counter electrode (CE), in contact with the NaCl-KCl molten salt, were used to measure the OCP after each addition. Notably, OCP values increased beyond 10 mol% $NiCl_2$, suggesting that higher $NiCl_2$ concentrations are required to achieve dual-phase behavior (liquid and solid) in the molten salt. This observation contradicts with the visual results, which indicated precipitates at 7.03 mol% $NiCl_2$ in solidified salts. However, the visual results are not reliable due to the lack of thermal control. The precipitates likely formed due to cooling, which reduces the concentration of $NiCl_2$ needed for saturation (See **Figure S2**).

According to the ternary phase diagram, more than 50 mol% $NiCl_2$ would be necessary to form a stable secondary phase at 1023 K (750 °C) operational temperature. However, due to the high vapor pressure of $NiCl_2$, the chloride salt easily volatilizes at elevated $NiCl_2$ concentrations, complicating electrochemical measurements in these conditions. The data was supported through thermogravimetric analysis (TGA) using a Netzsch STA 449F5 stored inside the glovebox, where $NiCl_2$ was analyzed over a temperature range from 313 K (40 °C) to 1273 K (1000 °C) at a heating rate of 20 °C/min under an argon flow rate of 240.3 ml/min. The results, shown in **Figure S5a**, indicate that $NiCl_2$ begins to sublimate at temperatures above 1023 K, evidenced by the formation of crystals within the TGA apparatus.

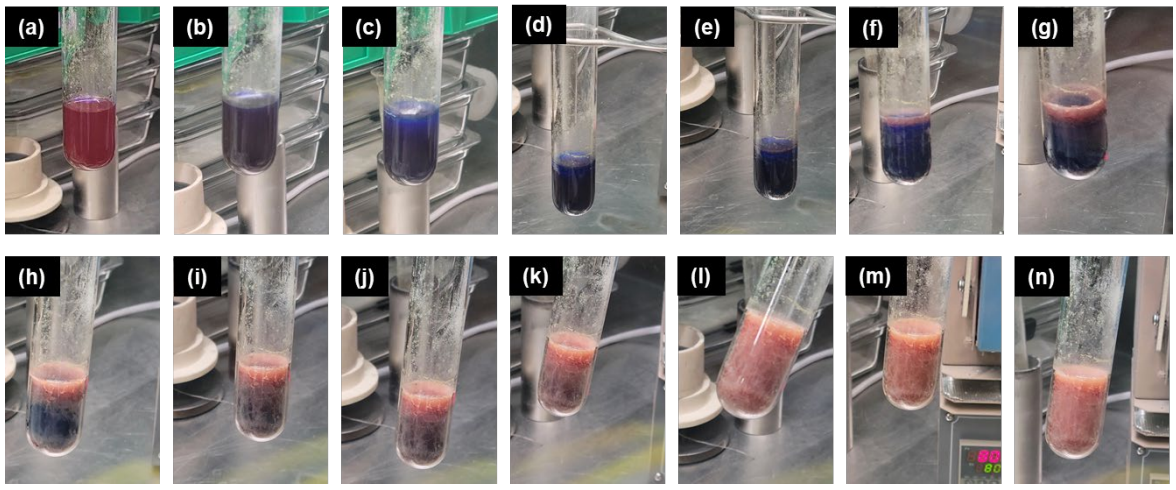

Figure S3. Thermal chromic transition temperature of molten salts containing 99.5 mol% equimolar NaCl-KCl and 0.5 mol% $NiCl_2$ at different time frames when first heated up to 1073 K and let it cool down to ambient temperature in a quartz test tube. **(a)** 0 s, **(b)** 20 s, **(c)** 40 s, **(d)** 1 min, **(e)** 1 min 20 s, **(f)** 1 min 40 s, **(g)** 2 min, **(h)** 2 min 20 s, **(i)** 2 min 40 s, **(j)** 3 min, **(k)** 3 min 20 s, **(l)** 3 min 40 s, **(m)** 4 min, and **(n)** 4 min 16 s.

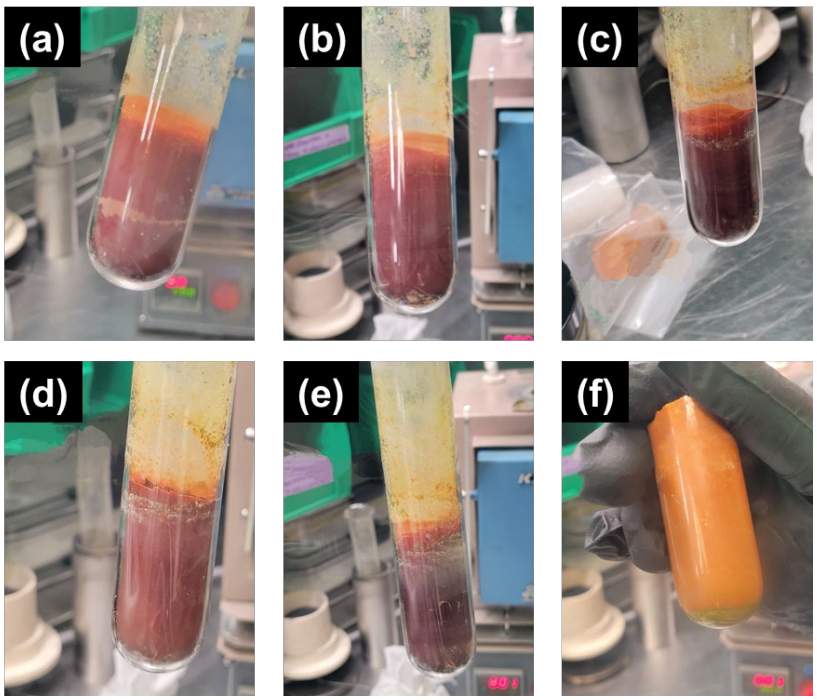

Figure S4. Visual determination of the saturation phase of $NiCl_2$ in NaCl-KCl by incrementally adding $NiCl_2$ to the molten salt mixture and allowing it to cool down. **(a)** 3.90 mol%, **(b)** 7.03 mol%, **(c)** 12.70 mol%, **(d)** 17.75 mol%, **(e)** 22.25 mol%, **(f)** 30.04 mol% of $NiCl_2$ in equimolar NaCl-KCl molten salt.

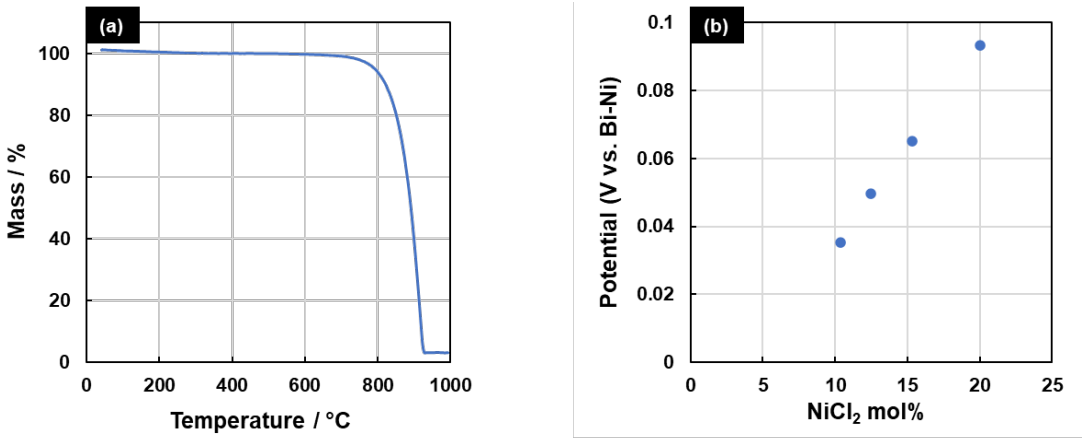

Figure S5. (a) TGA data of $NiCl_2$ and **(b)** OCP values at various mole fractions of $NiCl_2$ added to equimolar NaCl-KCl molten salt at 1023 K.

References

[1] A. Tanaka, H. Katayama, On the equilibrium diagram of system NaCl-KCl-NiCl2, Muroran Institute of Technology, 1970. http://hdl.handle.net/10258/3514.